Using gas-phase nitric acid as an indicator of PSC composition

Miriam von König, Holger Bremer, Armin Kleinböhl, Harry Küllmann and Klaus F. Künzi
Institute of Environmental Physics, University of Bremen, Bremen, Germany

Albert P.H. Goede
Space Research Organisation of the Netherlands (SRON), Utrecht, The Netherlands

Edward V. Browell and William B. Grant
Atmospheric Sciences Research, NASA Langley Research Center, Hampton, Virginia, USA

John Burris, Thomas McGee, and Laurence Twigg
NASA Goddard Space Flight Center, Greenbelt, Maryland, USA

Short title: HNO_3 AS INDICATOR OF PSC COMPOSITION

Abstract.

A combination of several airborne remote measurements – gas-phase HNO_3 measurements by the Airborne Submillimeter Radiometer ASUR, optical aerosol properties measured by the UV Differential Absorption Lidar DIAL and temperature measurements by the Airborne Raman Ozone, Temperature and Aerosol Lidar (AROTEL) – obtained during the SOLVE/THESEO2000 campaign during Arctic winter 1999/2000 are used to investigate the composition of polar stratospheric cloud (PSC) particles. A simple thermodynamical model is used to calculate the gas-phase amount of three possible PSC composites – nitric acid trihydrate (NAT), nitric acid dihydrate (NAD) and supersaturated ternary solutions (STS). The measured HNO_3 agrees very well with a NAT composition for two PSCs observed during a research flight on December 7, 1999. However, sensitivity studies show that while these PSCs are not in agreement with a STS composition, it is not possible to distinguish between a NAT and a NAD composition. By far the greatest contribution to the model uncertainty is due to uncertainties in the temperature data. Temperature data with an accuracy of better than 1 K are necessary to permit a distinction between NAT and NAD.

Introduction

Polar stratospheric clouds (PSCs) have been known to play a crucial role in stratospheric Arctic and Antarctic winter/spring ozone depletion for a long time (see e.g. [Peter, 1997; Solomon et al., 1999]). The heterogeneous reactions leading to chlorine activation, a prerequisite of ozone depletion, take place on the surfaces of solid stratospheric particles or in liquid stratospheric particles:

$$\begin{aligned} \mathrm{ClONO_2 + HCl} &\rightarrow \mathrm{Cl_2 + HNO_3} && \text{(1a)} \\ \mathrm{ClONO_2 + H_2O} &\rightarrow \mathrm{HOCl + HNO_3} && \text{(1b)} \\ \mathrm{HOCl + HCl} &\rightarrow \mathrm{Cl_2 + H_2O} && \text{(1c)} \\ \mathrm{N_2O_5 + H_2O} &\rightarrow \mathrm{2HNO_3} && \text{(1d)} \\ \mathrm{N_2O_5 + HCl} &\rightarrow \mathrm{ClNO_2 + HNO_3} && \text{(1e)} \end{aligned}$$

These reactions convert chlorine reservoir species like $ClONO_2$ and HCl into reactive and easily photolyzed species that can participate in catalytic ozone depletion cycles. Reactions (1a),(1b),(1d) and (1e) also form HNO_3 condensed in the particles and leads to an increase of the gas-phase amount of HNO_3 when the PSC evaporates.

PSCs are known to appear in two major compositions: below the ice frost point, ice particles will form (Type II PSCs). Type I PSCs form some K above the ice frost point and are believed to be condensates of HNO_3 and water. While the formation of Type II PSCs seems reasonably well understood, a considerable amount of uncertainty exists concerning the formation, as well as the composition, of Type I PSCs. Type I PSCs exist as solid condensates of HNO_3 and water (Type Ia) as well as in the form of supersaturated ternary solutions of HNO_3, H_2O and H_2SO_4 (STS, Type Ib) formed by cooling of the background aerosol [Carslaw et al., 1994; Tabazadeh et al., 1994]. Type Ia PSCs have first been suggested to be composed of nitric acid trihydrate NAT [Hanson and Mauersberger, 1988]. However, the formation of NAT particles still poses many unanswered questions. Different possibilities for the composition of PSC Type Ia have been proposed by some authors. For example, Worsnop et al. [1993] proposed nitric acid dihydrate (NAD, $HNO_3 \cdot 2H_2O$) as a possible composite for Type Ia PSCs.

All PSC composites – ice, STS and NAT/NAD – not only form at different temperatures, but also support different reaction rates for reactions (1a–1e). Therefore, the composition of the PSCs will not only determine the temperature below which chlorine activation occurs, but also the lifetime of the chlorine reservoir species in the presence of the PSCs. Thus, to know the composition and formation mechanism of PSC particles is a prerequisite to model ozone depletion accurately and to predict possible future ozone depletion. This is especially true for the Arctic winter, where temperatures are rarely below the ice frost point, and even temperatures below the NAT threshold occur infrequently and seldom for long periods of time.

Considering the importance of PSC composition for the determination of ozone depletion, very few direct measurements of this composition exist. The bulk of PSC measurements consist of measuring optical properties – e.g., particle backscatter ratio and depolarization. The first ever direct measurement of PSC composition occured as late as 1998, with a balloon borne mass spectrometer [Schreiner et al., 1999]. This instrument is to date the only instrument able to measure directly the composition of PSCs. It has flown successfully several times since 1998, most prominently during the SOLVE/THESEO2000 campaign [Voigt et al., 2000a,b].

We present an indirect method to determine the composition of Type I PSCs from a combination of optical PSC properties measured by the UV Differential Absorption Lidar (DIAL) [Browell et al., 1983; 1998], gas-phase HNO_3 mixing ratios measured by the Airborne Submillimeter Radiometer (ASUR), and temperature measurements obtained by the Airborne Raman Ozone, Temperature and Aerosol Lidar (AROTEL) [McGee et al., 2001]. A first approach to determine the PSC composition from the gas-phase amount of HNO_3 was presented already in 1990 [Schreiner and Arnold, 1990], using one HNO_3 profile measured by a rocket-borne instrument. Recently, Santee et al. [2001] used a combination of satellite measurements – POAM particle scatter and MLS HNO_3 profiles – to study PSC types and PSC formation during Arctic winter 1995/96. While satellite measurements have the advantage of greater coverage, the ASUR and DIAL measurements have been obtained with a very good horizontal resolution, which makes it possible to study the structure of individual PSCs.

Measurement of gas-phase HNO_3

HNO_3 was measured by the Airborne Submillimeter Radiometer ASUR. ASUR was developed for airborne measurements of stratospheric trace gases at the University of Bremen, in collaboration with the Space Research Organisation of the Netherlands (SRON). It was flown for the first time during the EASOE campaign in winter 1991/92 [Crewell et al., 1994]. It has been improved continously and has participated in a number of measurement campaigns during several Arctic winters [e.g. Wehr et al., 1995; Crewell et al., 1995; de Valk et al., 1997; von König et al., 2000]. Implementation of a liquid helium cooled SIS diode as the detector in 1994 has improved the signal-to-noise ratio by about a factor of fifteen [Mees et al., 1995]. The frequency range has been extended several times, increasing the number of measurable species. ASUR now covers the complete frequency range from 604.3 GHz to 662.3 GHz. This range includes lines of ClO, HCl, O_3, N_2O, HO_2, BrO, CH_3Cl, H_2O, and HNO_3. However, since the instrument instantaneous bandwidth is about 1.5 GHz, not all species can be measured simultaneously.

The lines measured are transitions from thermally exited rotational states, so measurements can be conducted independent of solar zenith angle. Measurements are affected solely by gas-phase species, not by solid or liquid phases. At the measured wavelength of about 0.5 mm, measurements are not affected by scattering from stratospheric particles. During the SOLVE/ THESEO2000 campaign, the instrument was mounted on the starboard side of the NASA DC-8 aircraft, measuring with a fixed elevation angle of 12 degrees.

The pressure broadening of the lines is used to derive altitude information from the measurements. Measured spectra are analysed using the Optimal Estimation Method described in detail i.e. in [Rodgers, 1976; 1990]. For HNO_3, vertical profiles of volume mixing ratio are retrieved on a 2 km altitude grid using a zero a priori profile. This leads to very smooth profiles with an altitude resolution of 6-10 km in the lower stratosphere, with the resolution decreasing to higher altitudes (see e.g. [Kleinböhl et al., 2001]). Spectra are integrated over approx. 100 s to achieve a sufficient signal to noise ratio. This leads to a horizontal resolution of about 20 km and a precision of about 0.3 ppb in the lower stratosphere. Sensitivity studies have been carried out to investigate the influence of systematic errors on the measurement. Several sources of possible systematic errors have been considered. The dominant source of systematic errors have been found to be the influence of nearby ozone lines and the calculation of the continuum, and an overall systematic error of 15 % or 0.6 ppb – whichever is larger – was estimated for the measurement accuracy. This value is confirmed by comparison with other HNO_3 profile measurements, i.e. with the MIPAS instrument and ground-based FTIR measurements [von König, 2001].

Measurements of December 7, 1999

In this paper, we focus on measurements from one flight during the first SOLVE deployment. On December 7, 1999, a flight was carried out to the Arctic islands of Franz-Josef-Land, Severnaya Semlja, and Spitzbergen. Around and north-east of Severnaya Semlja, a triangle was flown (see Figure 1). Temperatures had just fallen below the PSC threshold in the core of the polar vortex; the aim of this flight was to search for PSCs in the cold core of the polar vortex. Temperature measurements along the flight-track of the DC-8 show very low stratospheric temperatures during most of this flight (see Figure 2 A). Two PSCs were observed during this flight by the DIAL lidar (see Figure 2 B). These PSCs were observed during the first and third leg of the triangle, extending from 18 km to 24 km in altitude and over a horizontal range of several hundreds of kilometers. Both PSCs were identified by their optical properties as Type Ia PSCs, i.e. solid particles presumed to be NAT. Both show a similar, very distinct vertical structure, so it is safe to assume that this is the same cloud, crossed twice. HNO_3 was measured regularly by ASUR during this flight, with only short interruptions to tune to other molecules. A clear anticorrelation is observed between the lidar backscatter measurements and the ASUR HNO_3 measurements. During the PSC crossings, the gas-phase HNO_3 observed by ASUR decreases by about 3 ppb (Figure 2 C). Due to the restricted vertical resolution of ASUR, the vertical structure of the PSC is not reflected in the HNO_3 measurements. Rather, the decrease of HNO_3 is observed over a large vertical range from 17 km to 26 km.

Figure 1

Figure 2 A

Model

Model description

A simple model was developed to calculate gas-phase HNO_3 mixing ratios in thermodynamical equilibrium for three types of PSCs: nitric acid trihydrate, NAT, nitric acid dihydrate, NAD and supersaturated ternary solutions, STS. All three types consist of condensates of HNO_3 and water. Gas-phase mixing ratios were derived from the vapor pressures of the condensates. For the solid condensates, the HNO_3 equilibrium mixing ratio is a function of temperature, pressure and water vapor. The gas-phase equilibrium mixing ratio of the liquid depends on all major contents of the liquid, i.e. on H_2SO_4 and the amount of total HNO_3 as well as on temperature, pressure and water vapor. Total HNO_3 means the sum of gas-phase and condensed HNO_3. The HNO_3 mixing ratio for NAT was calculated according to Hanson and Mauersberger [1988], for NAD according to Worsnop et al. [1993], and for STS according to Carslaw et al. [1995].

Temperature and density were measured by the AROTEL lidar operating onboard the DC-8 [Burris et al., 2001]. Water vapor was assumed to increase from 4.75 ppm at about 60 hPa to 6.25 ppm at about 20 hPa altitude, in agreement with balloon measurements obtained during the SOLVE campaign [Schiller et al., 2001]. Values of total HNO_3 were estimated from ASUR measurements outside PSCs, taken during the same flight well inside the polar vortex. No measurements of H_2SO_4 were available. H_2SO_4 values of about 0.15 ppb were assumed, in agreement with SAGE II aerosol measurements for low aerosol loading. A summary of the model parameters and their values or sources is given in Table 1.

Table 1

HNO_3 mixing ratios were calculated for all locations and altitudes along the flight track where PSCs were observed by DIAL. PSC observations were defined by aerosol backscatter ratios larger than 0.6 in the infrared channel of the DIAL instrument. To minimize the influence of measurement noise, only grid-points for which the running mean of three neighbouring grid-points had IR aerosol backscatter ratios larger than 0.6 were used. This procedure yields model values of the HNO_3 mixing ratio with the vertical spacing of the DIAL data (about 75 m). To make these model profiles comparable to the measured HNO_3 values, the model profiles were embedded into the total HNO_3 profile extending from 10 km to 50 km altitude and smoothed to the ASUR altitude resolution. The subsequent steps of the model calculation and smoothing are shown in Figure 3 for the example of NAT. Figure 3

Model results and comparison with measurements

In Figure 3, the results of the model calculation are shown for the high-resolution profiles as well as for the model profiles on ASUR resolution for the example of NAT. Model results are shown over an altitude range of 16 km to 26 km, and are compared to the measured HNO_3 values over the same altitude range. In the high-resolution model run (Figure 3 A), HNO_3 values decrease from over 9.5 ppb to values of less than 1.5 ppb. The smoothed model profiles show a distinctive lower HNO_3 decrease (Figure 3 B). Values decrease from over 9.5 ppb outside the PSC to over 7.25 ppb during the first PSC observation, and over 6 ppb during the second PSC observation. The vertical structure is no longer reflected in the model profiles. Indeed, the smoothed model profiles for NAT show values and a horizontal variability very much like the measured HNO_3 (Figure 3 C), with very little vertical structure.

As both the modeled and measured smoothed profiles show very little vertical structure, mixing ratios from anywhere between 18 km and 24 km altitude show a similar behavior. In the following, only values from 22 km altitude are shown. It should be noted, however, that values from 18, 20 or 24 km altitude show a consistent behavior. In Figure 4, the evolution of the HNO_3 mixing ratio at 22 km Figure 4
altitude is shown during the PSC underflights. Shown are deviations from total HNO_3 for the measured values as well as for smoothed model results for NAT, NAD and STS. As already seen in Figure 3, the model results for NAT are in fairly good agreement with the measurement over large parts of the PSCs. Significant discrepancies between measurement and model only occur at the beginning of the second PSC underflight, where the modeled HNO_3 starts to decrease earlier than the measured HNO_3. The model results for NAD show significantly less variability than the measurement over most parts of the PSC observations. Only at the end of the first PSC observation and at the beginning of the second PSC observation – where the agreement with NAT is worst – is the modeled HNO_3 for NAD in reasonable

agreement with the measurement. The model results for STS show practically no variation during the complete modeled period; temperatures were apparently not low enough for the formation of STS.

Model sensitivity

The comparison of measured and modeled HNO_3 shows a reasonably good agreement assuming a NAT composition of the PSC. This is consistent with the lidar measurements which already showed that the PSC is not liquid. How significant is this result? Can we conclude from these results that the PSC is composed of NAT? To investigate this, the sensitivity of the model is tested for the parameters used as input for the calculation of gas-phase HNO_3: Temperature, H_2O, total HNO_3 and H_2SO_4.

Temperature. Temperature was measured by the AROTEL instrument using Raman scattering. As the observed PSCs are optically thin, measurements are not affected by scattering on the PSC particles. The statistical measurement error of the AROTEL measurement ranges from less than 1 K to values above 3 K, and generally increases with altitude (Figure 6). Here, the temperature error of the individual measurements was used.

Figure 6

H_2O. H_2O values are estimated from several balloon measurements taken during the SOLVE campaign [Schiller et al., 2001]. While qualitatively all measurements agree quite well, differences of up to 0.4 ppm are observed between the measurements. An error of 0.4 ppm is assumed for the H_2O data.

HNO_3. Total HNO_3 contributes to the model result in two ways: The gas-phase equilibrium mixing ratio of STS depends on total HNO_3; further, total HNO_3 is used for the smoothing of the high-resoluted model profiles. Values of total HNO_3 are estimated from ASUR measurements outside of PSCs, but inside the vortex. The accuracy of the ASUR measurements is about 15 % (see instrument description). A further error source could be the low vertical resolution of the measured HNO_3 profile. This could pose a serious problem if the HNO_3 profile was strongly structured, as during a PSC underflight or in situations with significant denitrification. As it was rather early in the winter, denitrification is very unlikely to have occured at that time. To quantify the influence of vertical resolution on the model results, model runs were carried out using three different profiles with different altitude resolutions. All three profiles give essentially the same profile if smoothed to the altitude resolution of the ASUR measurement. The unsmoothed profiles, however, show different peak altitudes, peak values and peak width (see Figure 5 A). The model results for the three different profiles are shown for the case of NAT in Figure 5 B. No significant differences can be observed between the three model runs, so the vertical resolution of the total HNO_3 profile is assumed not to contribute significantly to the model errors. A model error of 15 % is assumed for total HNO_3.

Figure 5 A

H_2SO_4. No measurements were available for H_2SO_4 mixing ratios. Values of about 0.15 ppb were assumed, varied between 0.02 ppb and 0.3 ppb; these variations had no substantial influence on the model results.

A summary of the estimated uncertainties of the model parameters is given in Table 1. Model runs have been conducted for all three types of PSCs, changing the input parameters by the estimated uncertainties. A total model error was calculated as square root of the quadratic sum of all model errors. Total model errors are shown in Figure 7 A-C, together with the model results, compared to the measurements. Even considering the total model errors, the PSC is not consistent with a STS composition (Figure 7 C). This result is in good agreement with the lidar measurements. A similarly clear distinction between a NAT and NAD composition is not possible. Considering the total errors, most of the PSC could be either NAT or NAD. An exception is only the first and thickest part of the PSC observed between 12:20 and 13:00 UT: this is very unlikely to be NAD, and so can be clearly identified as NAT (see Figure 7 A and B).

Figure 7 A-

What causes these large model errors? The dark grey areas in Figure 7 show the sum of the model errors *without the temperature uncertainties.* Now the errors are much smaller, in the range of, or even smaller than, the precision of the ASUR measurements. So, by far the largest contribution to the model errors come from uncertainties in the temperature data. In Figure 8, model results and errors are plotted assuming a temperature error of 1K. Now, a distinction between NAT and NAD would be possible at least in most parts of the PSC. It follows that temperature data with an accuracy of better than 1 K are neccessary to distinguish between the gas-phase HNO_3 amounts of NAT and NAD.

Figure 8

Summary and conclusions

The aim of this paper is to investigate the composition of polar stratospheric cloud particles using a combination of gas-phase HNO_3 measurements and lidar data. We used HNO_3 measurements taken by the Airborne Submillimeter Radiometer ASUR during one flight of the DC-8 research aircraft into the polar vortex on December 7, 1999, which were correlated with measurements of aerosol backscatter ratio measured simultaneously by the UV Differential Absorption Lidar DIAL. Two PSCs of Type Ia were observed by the lidar during this flight, and both PSC observations were correlated with a decrease of gas-phase HNO_3.

Model runs were carried out for three different compositions of Type I PSCs – NAT, NAD and STS – using temperature data measured by the Airborne Raman Ozone, Temperature and Aerosol Lidar AROTEL. Sensitivity studies for the model input parameters – temperature, H_2O, total HNO_3 and H_2SO_4 – were carried out, and the influence of the limited altitude resolution of the total HNO_3 profile was investigated. The smoothing of the total HNO_3 profile was shown to have a little influence on the model results. Systematic errors of H_2O, H_2SO_4 and total HNO_3 add up to a model error of about 0.4 ppb, in the order of magnitude of the measurement precision. A far larger impact on the model errors comes from temperature uncertainties.

Comparison of the model runs with the measured HNO_3 shows that these PSCs are in good agreement with a NAT composition, while NAD and especially STS compositions of the PSCs lead to a lower HNO_3 decrease over large parts of the PSC observations. Considering the estimated model errors, it is possible to show with these measurements that the PSCs are not composed of STS, in agreement with the Lidar data which show that the PSCs contain solid particles. The first part of the PSC is clearly composed of NAT; however, while the measurements agree better with a NAT composition of the PSCs, due to the large model errors caused by temperature uncertainties, for large parts of the PSCs a NAD composition cannot be ruled out completely. It was found that temperature data with uncertainties better than 1 K are neccessary to distuinguish between a NAT and NAD composition.

References

Browell, E.V., A.F. Carter, S.T. Shipley, R.J. Allen, C.J. Butler, M.N. Mayo, J.H. Siviter Jr., and W.M. Hall, NASA multipurpose airborne DIAL system and measurements of ozone and aerosol profiles, *Appl. Opt. 22*, 522-534, 1983.

Browell, E.V., S. Ismail, and W.B. Grant, Differential Absorption Lidar (DIAL) measurements from air and space, *Appl. Phys. B, 67*, 399-410, 1998.

Burris, J., McGee, T., Hoegy, W., Lait, L., Twigg, L., Sumnicht, G., Hostetler, C., Bui, T.P., Neuber, R., McDermid, I.S., Validation of Temperature Measurements from the Airborne Raman Ozone, Temperature and Aerosol Lidar During SOLVE, *J. Geophys. Res.,* , *this issue*, 2001.

Carslaw, K.S., B.P. Luo, S.L. Clegg, Th. Peter, P. Brimblecombe, and P.J. Crutzen, Stratospheric aerosol growth and HNO_3 gas phase depletion from coupled HNO_3 and water uptake by liquid particles, *Geophys. Res. Lett., 21*, 2479-2482, 1994.

Carslaw, K.S., B. Luo, and T. Peter, An analytic expression of aqueous HNO_3-H_2SO_4 stratospheric aerosols including gas phase removal of HNO_3, *Geophys. Res. Lett., 14*, 1877-1880, 1995.

Crewell, S., P. Hartogh, K.F. Künzi, H. Nett, and T. Wehr, Aircraft measurements of ClO and HCl during EASOE 1991/92, *Geophys. Res. Lett., 21*, 1267-1279, 1994.

Crewell, S., R. Fabian, K.F. Künzi, H. Nett, W. Read, J. Waters, and T. Wehr, Comparison of ClO measurements by airborne and spaceborne microwave radiometers in the Arctic winter stratosphere 1993, *Geophys. Res. Lett., 22*, 1489-1492, 1995.

Hanson, D., and K. Mauersberger, Laboratory studies of the nitric acid trihydrate: Implications for the south polar stratosphere, *Geophysical Research Letters 15*, 855-858, 1988.

Kleinböhl, A., et al., Vortexwide Denitrification of the Arctic Polar Stratosphere in Winter 1999/2000 determined by Remote Observations, *J. Geophys. Res.,* this issue, 2001.

von König, M., H. Bremer, V. Eyring, A. Goede, H. Hetzheim, Q. Kleipool, H. Küllmann, and K.F. Künzi, An airborne submm radiometer for the observation of stratospheric trace gases, in *Microwave Radiometry and Remote Sensing of the Earth's Surface and Atmosphere*, edited by

P. Pampaloni and S. Paloscia, VSP Utrecht, 2000a.

von König, M., Chlorine Activation and PSC Formation in the Arctic Stratosphere, Ph.D. Thesis, University of Bremen, Bremen, Germany, 2001.

McGee, T., Burris, J., Hoegy, W., Twigg, L., Sumnicht, G., Heaps, W., Hostetler, C., and Neuber, R., AROTEL: A DC-8 Lidar Instrument, In preparation, to be submitted to Applied Optics.

Mees, J., S. Crewell, H. Nett, G. de Lange, H. van den Stadt, J.J. Kuipers, and R.A. Panhuyzen, ASUR – An Airborne SIS receiver for Atmospheric Measurements of Trace Gases at 625 to 760 GHz, *IEEE Transactions on Microwave Theory and Techniques, 43*, 1995.

Peter, T., Microphysics and heterogeneous chemistry of polar stratospheric clouds, *Annual Rev. of Phys. Chem., 48*, 785-822, 1997.

Rodgers, C.D., Retrieval of atmospheric temperature and composition from remote measurements of thermal radiation, *Rev. of Geophys. and Space Physics 14*, 609-624, 1976.

Rodgers, C.D., Characterization and error analysis of profile retrieval from remote sounding measurements, *J. Geophys. Res.,* , *95*, 5587-5595, 1990.

Santee, M., A. Tabazadeh, G.L. Manney, M.D. Fromm, R.M. Bevilacqua, J.W. Waters, and E.J. Jensen, A Lagrangian approach to inferring the composition of Arctic polar stratospheric clouds from UARS MLS HNO_3 and POAM II aerosol extinction measurements, *J. Geophys. Res.,* , *submitted.*

Schiller, C., et al., Dehydration in the Arctic stratosphere during the THESEO2000/SOLVE campaigns, *J. Geophys. Res.,* , submitted to SOLVE special issue I, 2001.

Schlager, H., and F. Arnold, Measurement of stratospheric gaseous nitric acid in the Winter arctic vortex using a novel rocket-borne mass spectrometer method, *Geophysical Research Letters 17*, 433-436, 1990.

Schreiner, J., C. Voigt, A. Kohlmann, F. Arnold, K. Mauersberger and N. Larsen, Chemical analysis of polar stratospheric cloud particles, *Science 283*, 968-970, 1999.

Solomon, S., Stratospheric ozone depletion: A review of concepts and history, *Rev. of Geophys., 37*, 275-316, 1999.

Tabazadeh, A., R.P. Turco, and M.Z. Jacobson, A model for studying the composition and chemical effects of stratospheric aerosols, *J. Geophys. Res., 99*, 12897-12914, 1994.

de Valk, J.P.J.M.M., et al., Airborne Heterodyne Measurements of stratospheric ClO, HCl, O_3 and N_2O during SESAME-I over Northern Europe, *J. Geophys. Res., 102*, 1391-1398, 1997.

Voigt, C., et al., Nitric Acid Trihydrate in Polar Stratospheric Cloud Particles, *Science 290*, 1756, 2000a.

Voigt, C., A. Tsias, A. Dörnbrack, S. Meillinger, B. Luo, J. Schreiner, N. Larsen, K. Mauersberger, Non-equilibrium compositions of ternary polar stratospheric clouds in gravity waves, *Geophys. Res. Lett.*, , 27, 3873-3876, 2000b.

Wehr, T., S. Crewell, K.F. Künzi, J. Langen, H. Nett, J. Urban, and P. Hartogh, Remote Sensing of ClO and HCl over Northern Scandinavia in Winter 1992 with an Airborne Submillimeter Radiometer, *J. Geophys. Res., 100*, 20958-20968, 1995.

Worsnop, D.R., Fox, L.E., Zahniser, M.S., and Wofsy, S.C., Vapor Pressures of Solid Hydrates of Nitric Acid: Implications for Polar Stratospheric Clouds, *Science 259*, 71-74, 1993.

---

von König, M., Bremer, H., Kleinböhl, A., Küllmann, H. and Künzi, K. F., Institute of Environmental Physics, University of Bremen, Kufsteiner Strasse, 28359 Bremen, Germany. (miriam@env.leeds.ac.uk)

A.P.H. Goede, Space Research Organisation of the Netherlands, Utrecht, The Netherlands.

Browell, E. V., and Grant, W. B., NASA Langley Research Center, Atmospheric Sciences Research, MS 401A, VA 23681-2199, USA. (e.v.browell@larc.nasa.gov,
w.b.grant@larc.nasa.gov)

Burris, J., McGee, T., and Twigg, L., NASA Goddard Space Flight Center, Greenbelt, MD 20771, USA.

Received ______________________

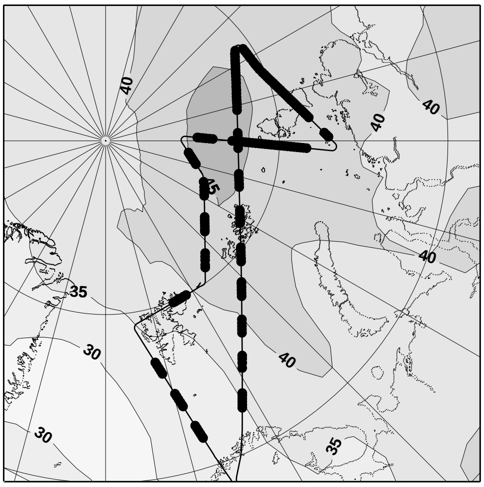

Figure 1. Flight track of the NASA DC-8 on December 7, 1999 (black line). Contours are ECMWF PV (in PVU) on the 475 K isentrope. Heavy black lines indicate portions of the flight when ASUR measured HNO_3. On the left hand side of the picture the coastline of north-east Greenland can be seen, coastlines in the bottom and right-hand side are the northern coast of Scandinavia and Siberia.

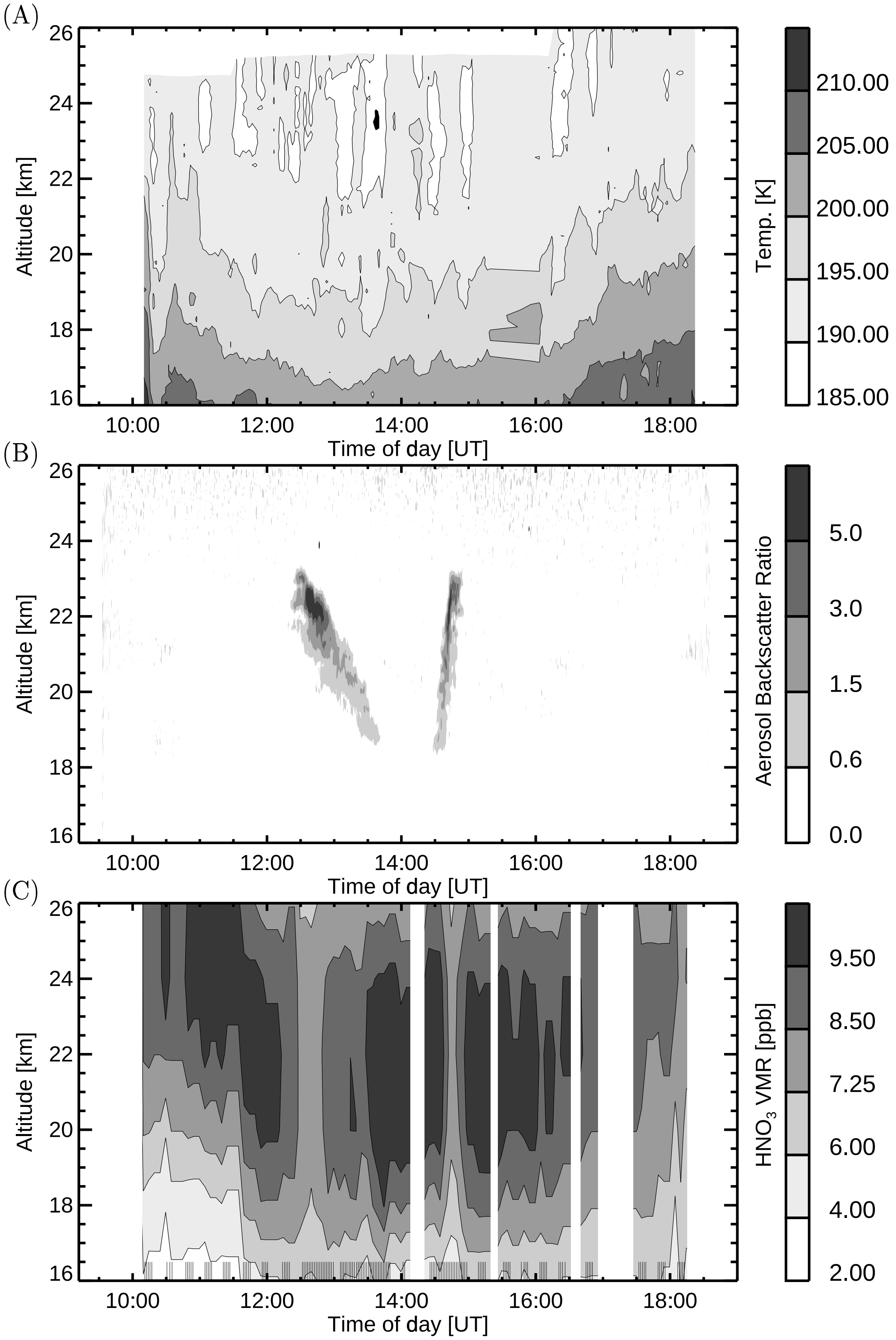
(A)
Altitude [km]
26
24
22
20
18
16
10:00
12:00
14:00
16:00
18:00
Time of day [UT]
Temp. [K]
210.00
205.00
200.00
195.00
190.00
185.00
(B)
Altitude [km]
26
24
22
20
18
16
10:00
12:00
14:00
16:00
18:00
Time of day [UT]
Aerosol Backscatter Ratio
5.0
3.0
1.5
0.6
0.0
(C)
Altitude [km]
26
24
22
20
18
16
10:00
12:00
14:00
16:00
18:00
Time of day [UT]
HNO_3 VMR [ppb]
9.50
8.50
7.25
6.00
4.00
2.00

Figure 2. Top: Temperature along the flight path of the NASA DC-8 on December 7, 1999, measured by the AROTEL instrument. Middle: Aerosol backscatter ratio at 1.06 μm, measured by the DIAL instrument during this flight. Two distinctive PSCs are observed, one from around 12:15 UT to around 13:45 UT, the other from 14:30 UT to around 15 UT. Bottom: Gas-phase HNO_3 mixing ratio measured by ASUR during the same flight. White spaces denote times when the ASUR instrument was tuned to other molecules. The measurements have been binned over five minute periods for greater clarity. A decrease of gas-phase HNO_3 of about 2 ppb is observed, clearly correlated to the lidar PSC observations.

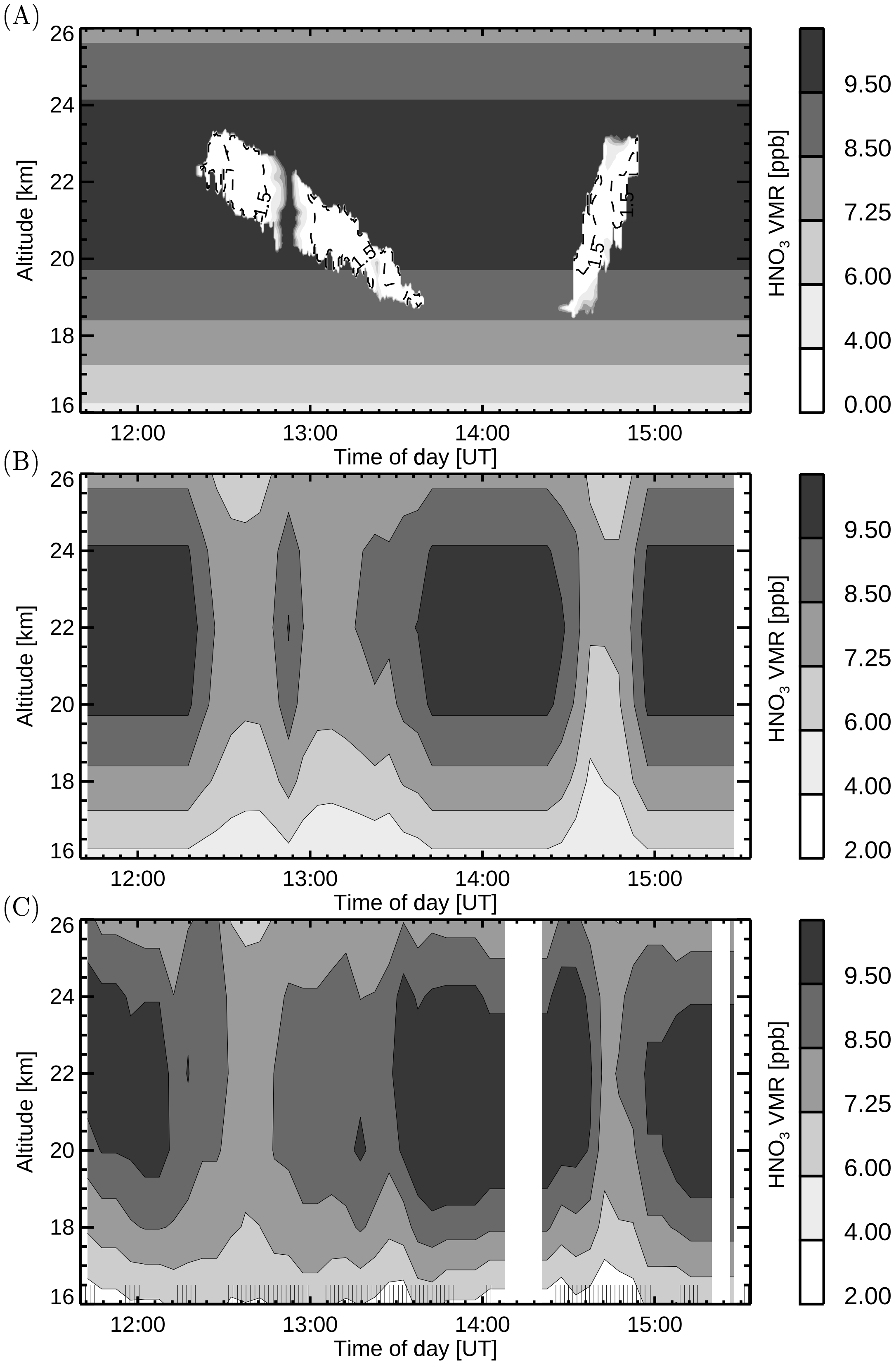
(A)
26
24
22
20
18
16
Altitude [km]
12:00
13:00
14:00
15:00
Time of day [UT]
1.5
1.5
1.5
HNO$_3$ VMR [ppb]
9.50
8.50
7.25
6.00
4.00
0.00
(B)
26
24
22
20
18
16
Altitude [km]
12:00
13:00
14:00
15:00
Time of day [UT]
HNO$_3$ VMR [ppb]
9.50
8.50
7.25
6.00
4.00
2.00
(C)
26
24
22
20
18
16
Altitude [km]
12:00
13:00
14:00
15:00
Time of day [UT]
HNO$_3$ VMR [ppb]
9.50
8.50
7.25
6.00
4.00
2.00

Figure 3. Model results for a NAT composition in comparison with measurements. Top: Calculated gas-phase mixing ratios of HNO_3 in equilibrium for a NAT composition, for all positions where PSCs were observed by DIAL. The HNO_3 values outside the PSC observations are total HNO_3 values derived from ASUR measurements without PSC coverage (see section Model description). Middle: the same model results, smoothed to ASURs altitude resolution. Bottom: ASUR measurement of gas-phase HNO_3 along the same flight track. Measurements and smoothed model results have been binned over five minute periods for greater clarity.

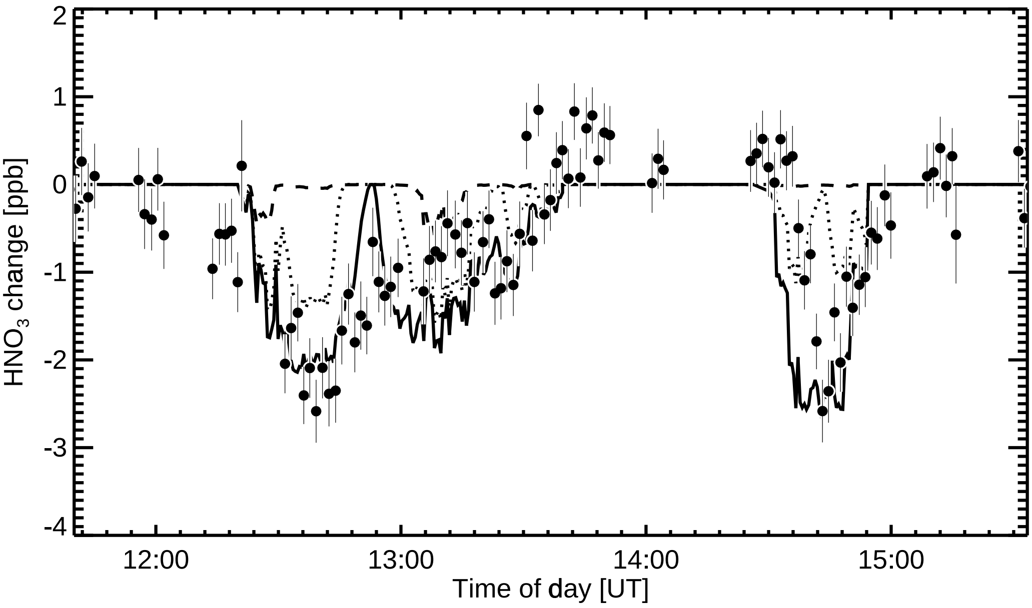

Figure 4. Model results for NAT (solid line), NAD (dotted line) and STS (dashed line) at 22 km altitude. Black dots are ASUR measurements at 22 km altitude. Error bars show the statistical 1 σ measurement error.

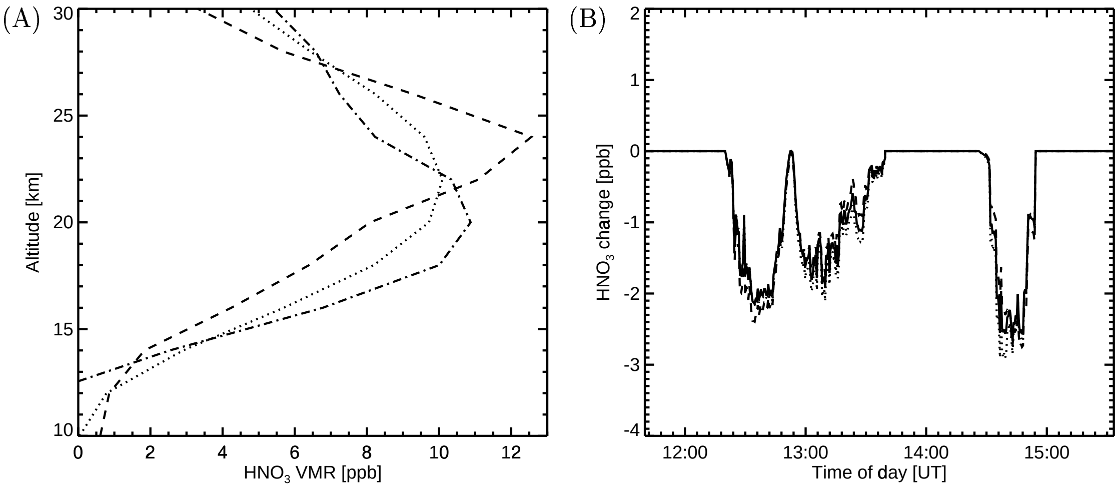

Figure 5. The sensitivity of the model results to the vertical resolution of total HNO_3. Left: three HNO_3 profiles with different peak altitudes, peak values and peak width, but similar column amounts. All three profiles yield the total HNO_3 profile used for the model calculations when smoothed to the ASUR vertical resolution. Right: Model runs for the case of a NAT composition for the three HNO_3 profiles shown in the left-hand plot at 22 km altitude.

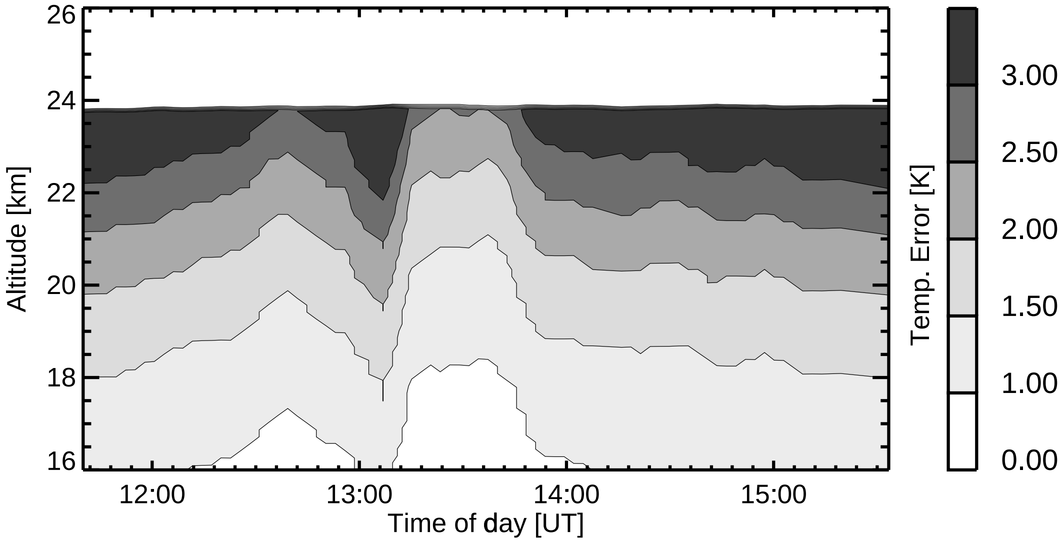

Figure 6. Uncertainty of the AROTEL temperature data along the flight-path of the DC-8

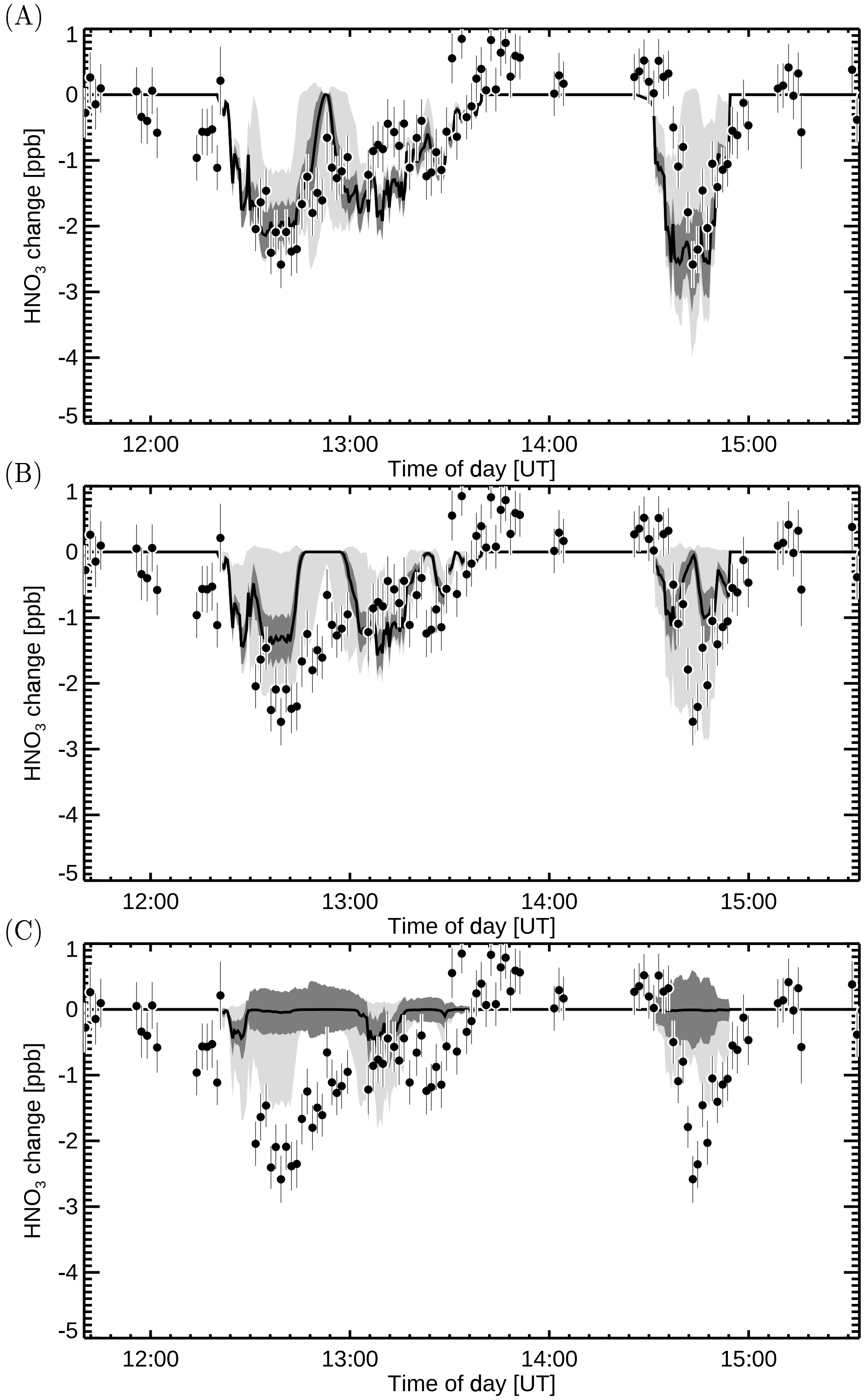
(A)
1
0
-1
-2
-3
-4
-5
HNO$_3$ change [ppb]
12:00
13:00
14:00
15:00
Time of day [UT]
(B)
1
0
-1
-2
-3
-4
-5
HNO$_3$ change [ppb]
12:00
13:00
14:00
15:00
Time of day [UT]
(C)
1
0
-1
-2
-3
-4
-5
HNO$_3$ change [ppb]
12:00
13:00
14:00
15:00
Time of day [UT]

Figure 7. Model sensitivity for NAT (top), NAD (middle) and STS (bottom), for 22 km altitude. Lines correspond to the model base results (see Figure 4). Light grey area: total model errors considering errors in temperature, water vapour, total HNO_3 and H_2SO_4 (the latter for STS only). Dark grey area: the same, but without the contribution of temperature errors. Black dots and error bars as in Figure 4.

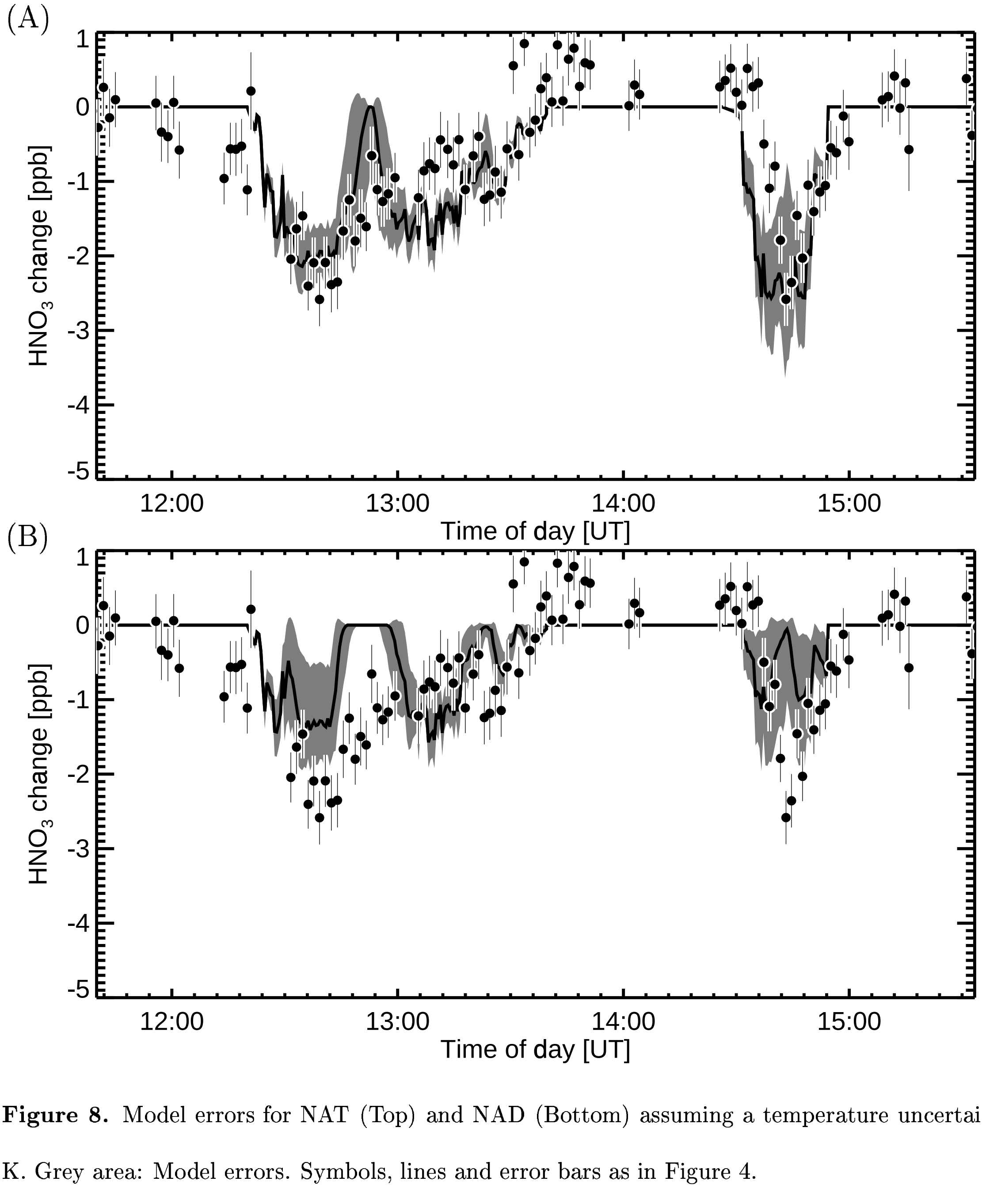

Figure 8. Model errors for NAT (Top) and NAD (Bottom) assuming a temperature uncertainty of 1 K. Grey area: Model errors. Symbols, lines and error bars as in Figure 4.

Table 1. Parameters used for the modeling of gas-phase HNO_3 and their assumed uncertainties.

Parameter	Value/source	Uncertainties
Temperature	AROTEL	see Figure 6
H_2O	4.75-6.25 ppm[a]	0.4 ppm
total HNO_3	ASUR[b]	15 %
H_2SO_4	0.15 ppb	0.02-0.3 ppb

[a] Altitude dependent.

[b] Total HNO_3 is derived from ASUR measurements of the same day, but without PSC coverage.